Integration of Local Inputs in Visual Cortex

Louis J. Toth[1], Dae-Shik Kim[2], S. Chenchal Rao and Mriganka Sur

Department of Brain and Cognitive Sciences, Massachusetts Institute of Technology, Cambridge, MA 02139, USA
[1]Present address: Department of Neurobiology, Harvard Medical School, 220 Longwood Avenue, Boston, MA 02115, USA
[2]Present address: Laboratory for Neural Modeling, Frontier Research Program, The Institute of Physical and Chemical Research (RIKEN), Wako-shi, Japan

In mammalian visual cortex, local connections are ubiquitous, extensively linking adjacent neurons of all types. In this study, optical maps of intrinsic signals and responses from single neurons were obtained from the same region of cat visual cortex while the effectiveness of the local cortical circuitry was altered by focally disinhibiting neurons within a column of known orientation preference. Maps of intrinsic signals indicated that local connections provide strong and functional subthreshold inputs to neighboring columns of other orientation preferences, altering the observed orientation preference to that of the disinhibited column. However, measuring the suprathreshold response using single-cell recordings revealed only mild changes of preferred orientation over the affected region. Because strongly tuned subthreshold inputs from cortex only marginally affect the tuning of a cortical cell's output, it is concluded that local cortical inputs are integrated weakly compared to geniculate inputs. Such circuitry potentially allows for the normalization of responses across a wide range of input activity through local averaging.

Introduction

The mammalian cerebral cortex is characterized by plexi of local and long-range connections (Peters and Jones, 1984). Long-range connections within early visual cortical areas (axonal processes traversing over 1 mm of the cortical surface) link widespread cortical regions of similar orientation preference (Rockland and Lund,1982; Gilbert and Wiesel, 1989; Katz and Callaway, 1990). These connections appear to be important for context-dependent modulation of responses, in particular by stimuli outside the classical receptive field (Gilbert and Wiesel, 1990; Knierim and VanEssen, 1992; Toth *et al.*, 1996). In comparison, the function of local connections in visual cortex (connections within 1 mm of a cell) remains largely unknown. Anatomically, these connections arise from all cell types in cortex (Ahmed *et al.*, 1994), target dendritic spines and shafts (Anderson *et al.*, 1994a), and include predominantly excitatory but also inhibitory synapses (Anderson *et al.*, 1994b). In slices prepared from developing as well as mature visual cortex, local connections provide strong excitation and inhibition to both pyramidal and inhibitory interneurons (Dalva and Katz, 1994). Furthermore, recordings from nearby pairs of visual cortical neurons demonstrate clear excitatory connections between spiny stellate cells (Stratford *et al.*, 1996; see also Markram and Tsodyks, 1996). Functionally, it remains unclear whether local connections in visual cortex are confined to a particular orientation column or span a wide range of orientations, and if the latter, what their role in shaping cortical responses might be. In this study, the role of local connections in area 18 of cat visual cortex is examined using a novel combination of single-unit recording and intrinsic signal imaging during focal iontophoresis of bicuculline. Preliminary data has been published in abstract form (Toth *et al.*, 1995).

Materials and Methods

Adult cats (n = 5) were anesthetized initially with ketamine (15 mg/kg) and xylazine (1.5 mg/kg) i.m., and maintained with isofluorane (0.6–1.5% in 70/30 N_2O/O_2) delivered through a tracheal cannula. Cats were paralyzed with gallamine (3.6 mg/h) to prevent eye-movements and artificially respired to maintain end-tidal CO_2 at a partial pressure of 30 ± 3 mmHg. EEG and heart rate were continuously monitored to ensure adequate anesthesia. Craniotomies centered at the Horsley–Clark A3 coordinate allowed superficial access to a large portion of area 18. Moving square-wave gratings (spatial frequency 0.15 cycles/deg, temporal frequency 2 cycles/s, eight orientations separated by 22.5°, in both directions of motion) were shown on a 17-in. monitor (Sony Trinitron, 640 × 480, 60 Hz) positioned 30 cm in front of the animal. Grating contrast was 99%; neutral gray intensity was 6.0 cd/m^2.

Imaging Technique

Intrinsic signal imaging, a technique based on the spatial localization of sites of activity-dependent oxyhemoglobin reduction, was performed as follows. Images were obtained from a depth of 300–500 μm under 600 nm light (10 nm bandwidth), using a tandem-lens macroscope arrangement (Ratzlaff and Grinvald, 1991) giving an overall magnification of 75 pixels/mm. Images were collected using a Bischke CCD-5024N video camera at a 655 × 480 resolution without binning, and digitized by an Imager2001 system (Optical Imaging Inc., Durham NC) and a 486–66 PC with a Matrox graphics board. Frames were summed between 1.3 and 4.0 s after the onset of stimulus motion, corresponding to the time of maximum signal as determined by our previous experiments. Data was analyzed using programs written by the authors (L.J.T., S.C.R.) using C++ (Borland) or IDL (Research Systems Inc., Boulder CO). Out-of-focus regions and regions containing strong blood-vessel artifacts were masked for purposes of data analysis. No spatial filtering of the images was performed.

Iontophoresis

Bicuculline methiodide (20 mM, pH 3.0, Sigma) was injected using an iontophoresis unit (Medical Systems) at varying cathodic currents (see text) through a filamented, borosilicate glass pipette pulled to a tip size of 5 μm, and positioned 200–400 μm beneath the surface at the start of the experiment. A retention current of –10nA was applied during initial and recovery periods. Pipette and electrode positions were recorded visually relative to the surface vasculature using the imaging camera. Signals were summed over 40–60 stimulus presentations, occupying ~2 h of recording time per condition. Responses to both directions of motion were summed to obtain the response at one orientation. Waiting periods of 5–10 min after the start of iontophoresis and 20–30 min after cessation were used to ensure a steady-state condition during imaging.

Single-unit Recording

Single-unit responses to computer-generated high-contrast moving bars (16 directions, 8 repetitions) were recorded using electrodes of 2–5 MΩ impedance (MicroProbe Inc., Hagerstown, MD). Optimal length, width and velocity were determined for each cell. Spikes were windowed spatially and temporally (PSD-1, Harvard Apparatus) to ensure that all responses were from single cells. Data collection took ~2 h for each condition: initial, during bicuculline iontophoresis (20 mM, +93 nA), and recovery. Extracellular recordings were played through an audio monitor,

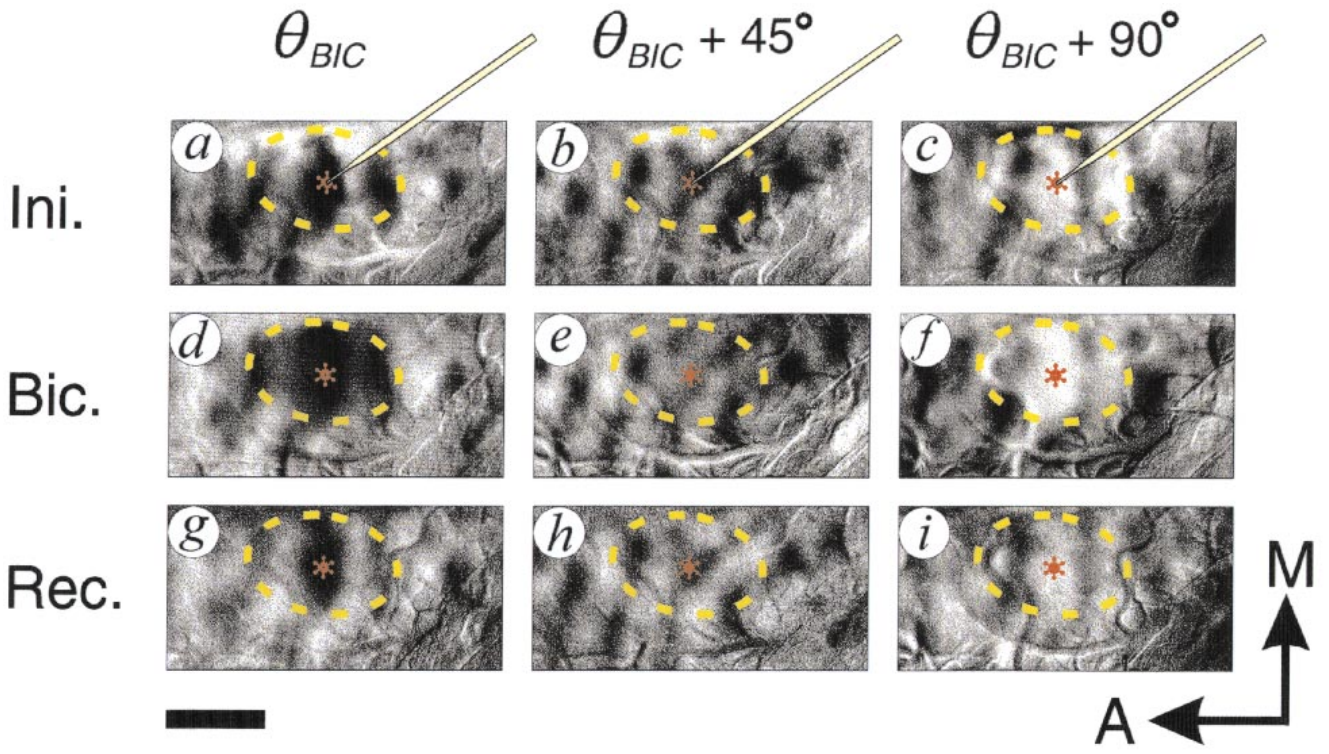

Figure 1. Single condition maps show the effect of bicuculline iontophoresis on visually evoked responses to oriented grating stimuli in cat area 18. Rows represent data obtained before (*a*,*b*,*c*), during (*d*,*e*,*f*) and after (*g*,*h*,*i*) iontophoresis of bicuculline (93 nA), and columns represent stimulus orientations equal (θ_{BIC}; *a*,*d*,*g*), oblique ($\theta_{(BIC+45)}$; *b*,*e*,*h*) and orthogonal ($\theta_{(BIC+90)}$; *c*,*f*,*i*) to that of the pipette region. The location of the pipette in each panel is indicated by a star. During iontophoresis, the area of cortex responsive to orientation θ_{BIC} increases dramatically (*d*, dashed yellow line indicates approximate extent). Activity for orthogonal orientations decreases (*f*), while that for other orientations remains largely unchanged (*e*). Scale bar: 1 mm. A: anterior, M: medial.

and displayed on-line to confirm the presence of a bicuculline effect and the adequacy of the waiting periods. For analysis, only cells which exhibited a recovery of their initial orientation vector were included. Orientation index was calculated using the formula:

$$OI = [(R_{BIC} - \text{avg}(R_{BIC+90} + R_{BIC-90})]/[(R_{BIC} + \text{avg}(R_{BIC+90} + R_{BIC-90})]$$

Direction index was calculated using the formula:

$$DI = [(R_{BIC} - (R_{BIC+180})]/[(R_{BIC} + (R_{BIC+180})]$$

where the subscript indicates the stimulus direction that evoked response R in single-unit recordings. θ_{BIC} = orientation preference at injection site, $\theta_{(BIC \pm 90)}$ = orientation orthogonal to injection site preference at both directions of motion, $\theta_{(BIC+180)} = \theta_{BIC}$ orientation with reverse direction of motion.)

Results

To examine the spread of local signals and their role in cortical function, we used a combination of intrinsic signal imaging and single-unit recording in cat visual cortex during focal iontophoresis of the $GABA_A$ antagonist bicuculline ('focal disinhibition'). A micropipette was introduced into layer II/III of cat area 18, and intrinsic signal maps were recorded for several millimeters around it (Fig. 1). Dark regions in these single-condition maps indicate areas of high, stimulus-specific activity in response to a particular stimulus orientation. These maps

Figure 2. Vector angle maps (*a*) prior to focal disinhibition, (*b*) during focal disinhibition and (*c*) after recovery are shown for the same experiment as in Figure 1. The map in (*a*) is obtained with the pipette in position (at the starred location) and retention current applied. During bicuculline iontophoresis (*b*), the normal orientation map in the region around the pipette is altered, such that the initial orientation at the pipette location is drastically overrepresented. Recovery of the normal map upon cessation of iontophoresis is shown in (*c*). Scale bar: 1 mm. Anterior, medial directions as in Figure 1. To produce the vector angle map, imaging data was treated vectorially by assigning each pixel of the 16 single-condition maps a magnitude representing the strength of the signal, and an angle representing 2× the orientation of the inducing stimulus. The 16 vectors at each pixel were added, and the resultant vector angle shown by the color-code at the bottom of the figure. (*d*) shows that the shift in orientation occurs in columns spanning all possible initial orientations. (*x*-axis represents the difference in vector angles taken pixel-by-pixel in the original images, and binned for clarity.) The solid curve shows the orientation shift within the affected region in map (*b*) minus map (*a*), and dashed line shows the recovery of the same region to initial values in (*c*) minus (*a*). The analyzed region is bounded by the ellipse in Figure 1 and includes 30 793 pixels (18% of image). A strong shift to the θ_{BIC} orientation is seen across all initial values of orientation, nearby orientations changing relatively little, and orthogonal orientations changing nearly 90°, suggesting that areas of all orientation preference receive input from the starred orientation column.

Figure 3. Low and high doses of bicuculline cause differing effects on intrinsic signal maps. For each condition, the activity map (top) for the pipette orientation ($\theta_{BIC} = 75°$), and polar map (bottom) are shown. The polar map codes both angle (color, color key as in Fig. 2) and magnitude (brightness, highly orientation selective regions being more saturated) of orientation preference. (*a*) A high dose of bicuculline (200 nA, 20 mM) causes a uniform pattern of activity around the injection site which is roughly equivalent for all stimulus orientations. (*b*) Recovery of the same cortex after bicuculline administration shows normal orientation-specific responses, including the orientation column beneath the pipette. (*c*) A low dose of bicuculline (50 nA, 20 mM) causes a strong spread of activation (black region) specific to the 'pipette orientation' (75°, between yellow and orange), distinctly different from the effect observed in (a). The dashed outline is centered on the pipette position, and indicates the approximate extent of the bicuculline effect. Scale bar, 1 mm.

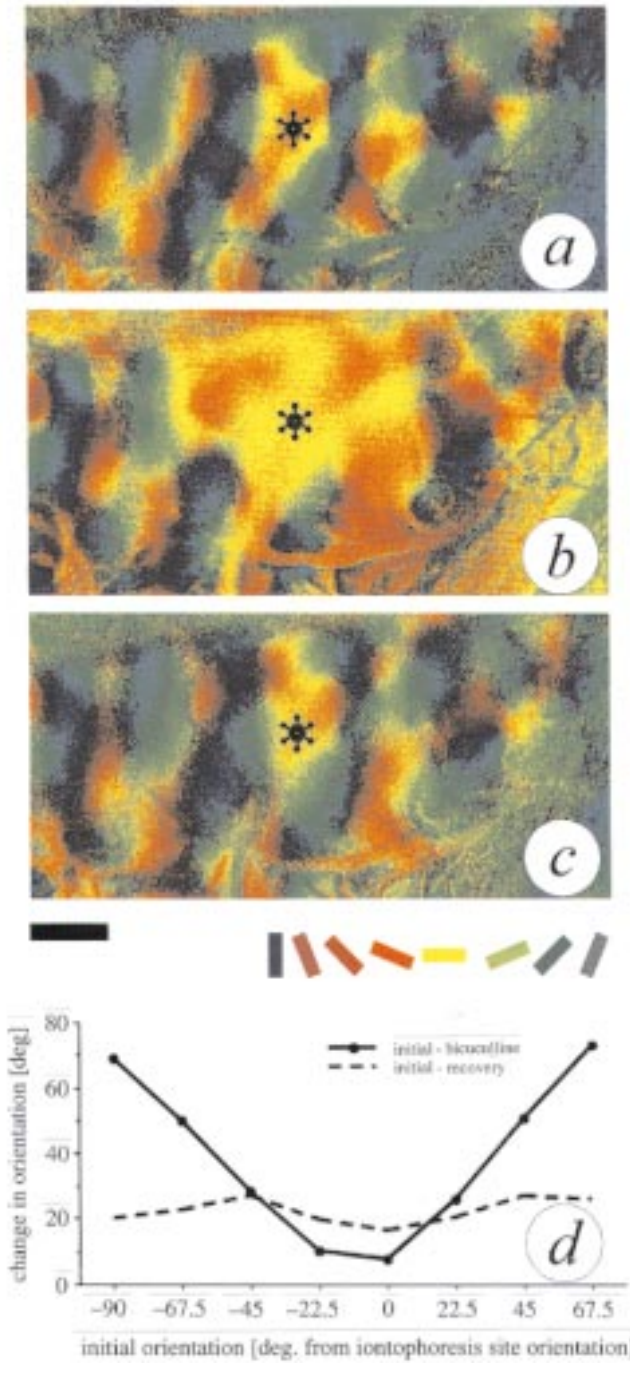

Figure 2.

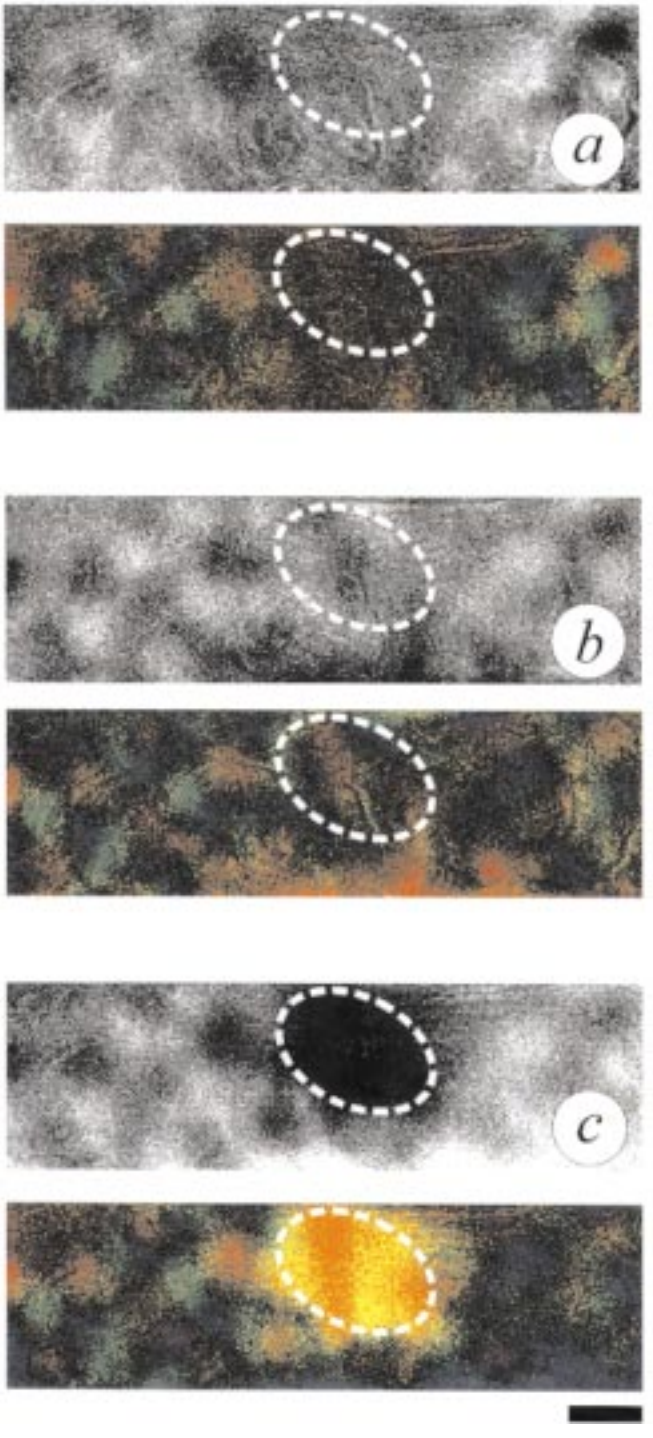

Figure 3.

show a normal, patchy distribution of orientation domains (Fig. 1*a–c*) with a center-to-center distance of ~1 mm, as has been seen in previous studies (Bonhoeffer and Grinvald, 1991). The iontophoresis pipette, which approaches from the posterior at a shallow angle, does not obscure the intrinsic signals, primarily due to (i) the shallow depth of field of the imaging optics, focused far from the shank of the pipette, and (ii) the fineness and transparency of the pipette tip. During focal disinhibition, single-condition maps show a profoundly altered pattern of activity (Fig. 1*d–f*). Figure 1*d* shows the map obtained for a stimulus orientation equal to the initial preferred orientation at the location of the pipette tip, referred to as θ_{BIC}. As expected, focal disinhibition raises the general level of activity for the preferred orientation, but surprisingly, the *area* of cortex responsive to orientation θ_{BIC} increases dramatically for regions up to 1.5 mm away from the injection location (marked with yellow, dashed line on Fig. 1). At greater distances, there is no obvious effect on the layout of orientation domains. The increase in responsiveness is also specific to the orientation preference immediately surrounding the pipette. Some loss of respon-

siveness to orthogonal stimuli can also be observed (Fig. 1*f*), though responsiveness to intermediate orientations is relatively unchanged (Fig. 1*e*). The general effect is an increased response across all orientation domains but only in response to stimuli of the θ_{BIC} orientation. This was the only effect found consistently across multiple experiments, though within a given set of maps, other changes may arguably be present, especially changes of signal magnitude. After the cessation of iontophoretic current, the original pattern of activation for all stimulus orientations returned (Fig. 1*g–i*). Iontophoresis with the incorrect polarity (as a control) did not alter the original pattern (data not shown).

Changes in orientation preference are more clearly observed using a composite map of the orientation vector angle (see legend to Fig. 2). In these maps, the preferred stimulus angle is indicated by the rainbow color coding shown in the key. The initial angle map (Fig. 2*a*) shows that the pipette was placed into a region of orientation preference (θ_{BIC}) coded by orange. Focal disinhibition (Fig. 2*b*) causes the region around the pipette to become dominated by nearby orientations (coded by orange and yellow). The θ_{BIC} orientation domain in Figure 2*b* extends a maximum of 1.5 mm radially from the pipette (average radius 1.1 mm). Within this region (dashed line, Fig. 1), orientation singularities ('pinwheels') disappear and the normal structure of orientation domains is profoundly altered. Orientation preference is homogenous. Within the affected region, the correlation coefficient across orientation is 0.054, suggesting weak or no correlation, while outside the affected region, orientation preferences are unchanged (correlation coefficient = 0.896). Neurons of all initial orientations, even those orthogonal to θ_{BIC}, are affected, as shown by the plot of shift in vector angle vs. initial vector angle in Figure 2*d*. Interestingly, the affected region approximately spans the distance from the pipette to the nearest neighbor iso-orientation domains. The vector angle map obtained after cessation of iontophoresis (Fig. 2*c*) is almost identical to the initial map (compare Fig. 2*a* with 2*c*). While there is some constant amount of difference between initial and recovery orientation maps, there is no significant difference between the comparison of regions near to (<1.0 mm) or far from (>1.5 mm) the pipette, demonstrating that the disinhibition is reversible and that the cortex remained healthy for the duration of recording. The constant difference between initial and recovery maps may be attributed perhaps to tiny positional shifts during the 2–6 h interval between data collection, or perhaps to local changes in cortical reflectivity due to minor variations in quality of blood or cerebrospinal fluid perfusion.

Bicuculline is known to have dose-dependent effects, and to precipitate several distinct modes of epileptiform behavior as dose is increased (Chagnac-Amitai and Connors, 1989). Such an activity pattern is seen in Figure 3*a*, obtained while a high dose of bicuculline was applied at the center of the encircled region. Epileptiform activity is seen in the intrinsic signal image as an absence of orientation column patterning in the raw data, and a black area in the polar map indicating no orientation preference to the evoked activity in that region (see legend to Fig. 3). Normal orientation-specific activity could again be obtained in this region after several hours (Fig. 3*b*). By contrast, low-dose bicuculline (Fig. 3*c*) caused a local, strongly orientation-specific effect similar to the other examples shown in Figures 2*b* and 5*b*,*d*. Single-unit recordings confirmed the absence of gross epileptiform activity under low doses of bicuculline (see below). Other than the three modes of activity shown in Figure 3, no strong dose-dependencies were observed, suggesting that these three modes represent different fundamental states of the underlying neural circuitry.

If bicuculline is indeed acting focally and specifically to disinhibit a cortical column, one prediction is that *increasing* the inhibition to a column, for example by iontophoresis of the inhibitory transmitter GABA itself, would lead to the opposite effect, namely a *shrinking* of the area preferring the θ_{GABA} orientation over the same 1.5 mm radius region. Direct iontophoresis of the neurotransmitter GABA under the same paradigm did in fact cause an underrepresentation of θ_{GABA} over a comparably sized region of cortex (compare Fig. 4*a* and *b*) which was also reversible (Fig. 4*c*). The profile of the orientation shifts induced by GABA (Fig. 4*d*) is roughly the inverse of that produced by bicuculline (Fig. 2*d*), though the magnitude of the effect is somewhat weaker, as might be expected since GABA also lessens the overall cortical response.

Several other observations also suggest that low-dose bicuculline in this preparation is acting focally and specifically. First, single-condition images of the stimulus-evoked activity for orientations different from θ_{BIC} appear normal (Fig. 1*e*,*f*). If bicuculline were spreading non-specifically over the cortical surface, one would expect to observe increased intrinsic signals also for orientations different from θ_{BIC}. One would also expect that the shifts in single-unit orientation would be larger for units closer to the pipette; however, no such correlation is observed (see Fig. 5*e* and below). Also, single-unit recordings even within 400 μm of the injection site show only minimal evidence of the classical effects of bicuculline. These cells give reliable stimulus-evoked responses, without showing evidence of non-specific, epileptiform activity associated with more drastic manipulations of the inhibitory circuitry (Kamphuis and Lopez da Silva, 1994).

Since it has been shown that subthreshold activity can make a large contribution to intrinsic signal responses (Toth *et al.*, 1994, 1996; Das and Gilbert, 1995), single-unit recordings were necessary to ascertain to what degree the observed effects were reflected in the actual neuronal spiking. Therefore, the correlation between the imaged vector angle map and the orientation preference of single-units recorded within the affected region of cortex during focal disinhibition was examined.

Two typical examples of single-unit responses (from two different experiments) are shown as polar plots in Figure 5*a*,*c*. Angle maps in Figure 5*b*,*d* show the position of the recorded neurons relative to the site of disinhibition and the range of the intrinsic signal effect. Observed over the population of single-units recorded are increases in tuning width (average change in orientation index = 0.18, see legend to Fig. 5 for method), increases in spontaneous activity (average change = 2.1 spikes/s), and a reduction of direction selectivity (average change in direction index = 0.13), consistent with known effects of low doses of bicuculline (Sillito, 1975, 1977, 1979). In most cells, relatively little change in preferred orientation is observed during bicuculline iontophoresis (compare colored curves with black curves in Fig. 5*a*,*b*). However, calculating vector angle in an analogous manner to the calculation of the intrinsic signal vector angle map reveals subtle but consistent shifts in orientation preference of the recorded units (average shift = 8.8°, θ = 5.96°, n = 13). Over the entire population, it is significant that every shift occurs in the predicted direction ($P <$ 0.01, sign test); that is, under conditions of focal disinhibition, all neurons adopt a new orientation preference closer to θ_{BIC} (see Fig. 5*e*). These single-unit data confirm, in several points, the results we obtained using intrinsic-signal imaging. Since

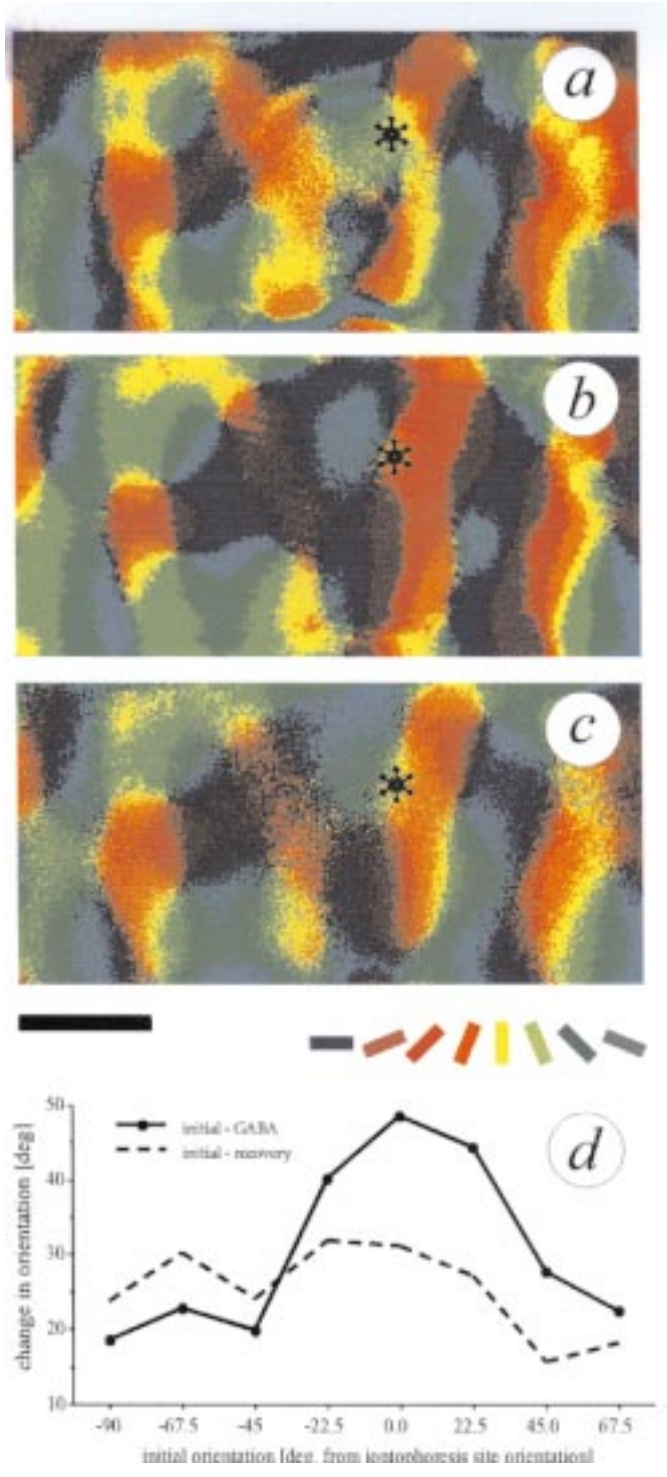

Figure 4. Vector angle maps (*a*) of the initial state, (*b*) during focal increase of inhibition with GABA and (*c*) after recovery are shown (in a different animal from that shown in Fig. 3). The map in (*a*) is obtained with the pipette in position (at the starred location) and retention current applied. GABA iontophoresis (93 nA) (*b*) causes an opposite effect to that of bicuculline; the normal orientation map in the region around the pipette is altered such that the initial orientation at the pipette location is drastically underrepresented. Yellow orientation columns are much reduced and the orthogonal, blue columns are much expanded within 1–1.5 mm around the pipette, but relatively unchanged outside that radius. Recovery of the normal map upon cessation of iontophoresis is shown in (*c*). Scale bar: 1 mm. Anterior, medial directions as in Figure 1. (*d*) shows that the shift in orientation occurs in columns spanning all possible initial orientations; same method as Figure 2*d*. Analyzed region is 25 115 pixels around the pipette location (16% of total image). A strong shift *away* from the θ_{GABA} orientation is seen across all initial values of orientation, with like-orientations changing the most.

single-units consistently shift *towards* θ_{BIC}, responses to θ_{BIC} become overrepresented (as in Fig. 1*d*), and responses to $\theta_{(BIC + 90)}$ are reduced (as in Fig. 1*f*). The net population effect in both cases is an overrepresentation of the θ_{BIC} orientation (as in Fig. 2*b*), though the observed magnitude of orientation shift is much greater in the intrinsic signal data.

Discussion

The intrinsic signal imaging data presented here suggest that local connections (i.e. connections within 1 mm of a neuron, or connections to neurons closer than those in neighboring iso-orientation columns) distribute information to columns of widely varying orientation preference. One can infer that the local connections are predominantly excitatory, since increasing their activity leads to an overrepresentation rather than a suppression of the tuning angle at the focus. Anatomical studies also support the prevalence of excitatory connections (Anderson *et al.*, 1994b). Although much is known about the physiology of long-range tangential connections, relatively little is known about signals carried by tangential, local connections. Long-range axons arise from excitatory neurons (Gilbert and Wiesel, 1989) and connect neurons of similar orientation preference (Gilbert and Wiesel, 1989; Weliky *et al.*, 1995; Das and Gilbert 1995; Toth *et al.*, 1996), though their ultimate effect may be excitatory or inhibitory (Weliky *et al.*, 1995; Toth *et al.*, 1996). A brief report examining the role of local connections in visual cortex (Dalva *et al.*, 1996) concluded that local inhibitory connections target neurons of all orientations. The results presented here are complementary to these data – by using bicuculline to block inhibition focally, our study demonstrates that the local excitatory effects also target neurons of all orientations.

These data do not contradict earlier single-unit studies of the effects of GABAergic compounds in visual cortex, involved neurons recorded at the site of bicuculline iontophoresis (Sillito, 1975, 1977, 1979), during global bicuculline application (Pettigrew and Daniels, 1973; Rose and Blakemore, 1974) or during focal GABA application within a local range (Crook and Eysel, 1992). The imaging data presented here demonstrate that the preferred orientation θ_{BIC} *at* the site of iontophoresis remains unchanged under bicuculline, in agreement with results from Sillito (1975, 1979). Furthermore, Crook and Eysel (1992), when applying GABA 500 μm away from the recorded single-units, noted changes in orientation preference for a significant percentage of cells. Although they did not record the direction of that change relative to the orientation preference of the inhibited area, we would predict the inverse result: orientation shifts that are consistently away from the orientation preference of the inhibited area.

Various functions have previously been proposed for local connections. The idea that specific inhibitory connections to cross-orientation columns are responsible for sharpening orientation selectivity has fallen into disfavor after whole-cell recordings *in vivo* failed to reveal cross-orientation inhibition (Ferster, 1986). Furthermore, intracellular blockade of inhibition was found to have no effect on orientation selectivity (Nelson *et al.*, 1994). Recent experiments indicate that the geometrical arrangement of receptive fields from the thalamic inputs correlates well with the orientation axis of cortical neurons

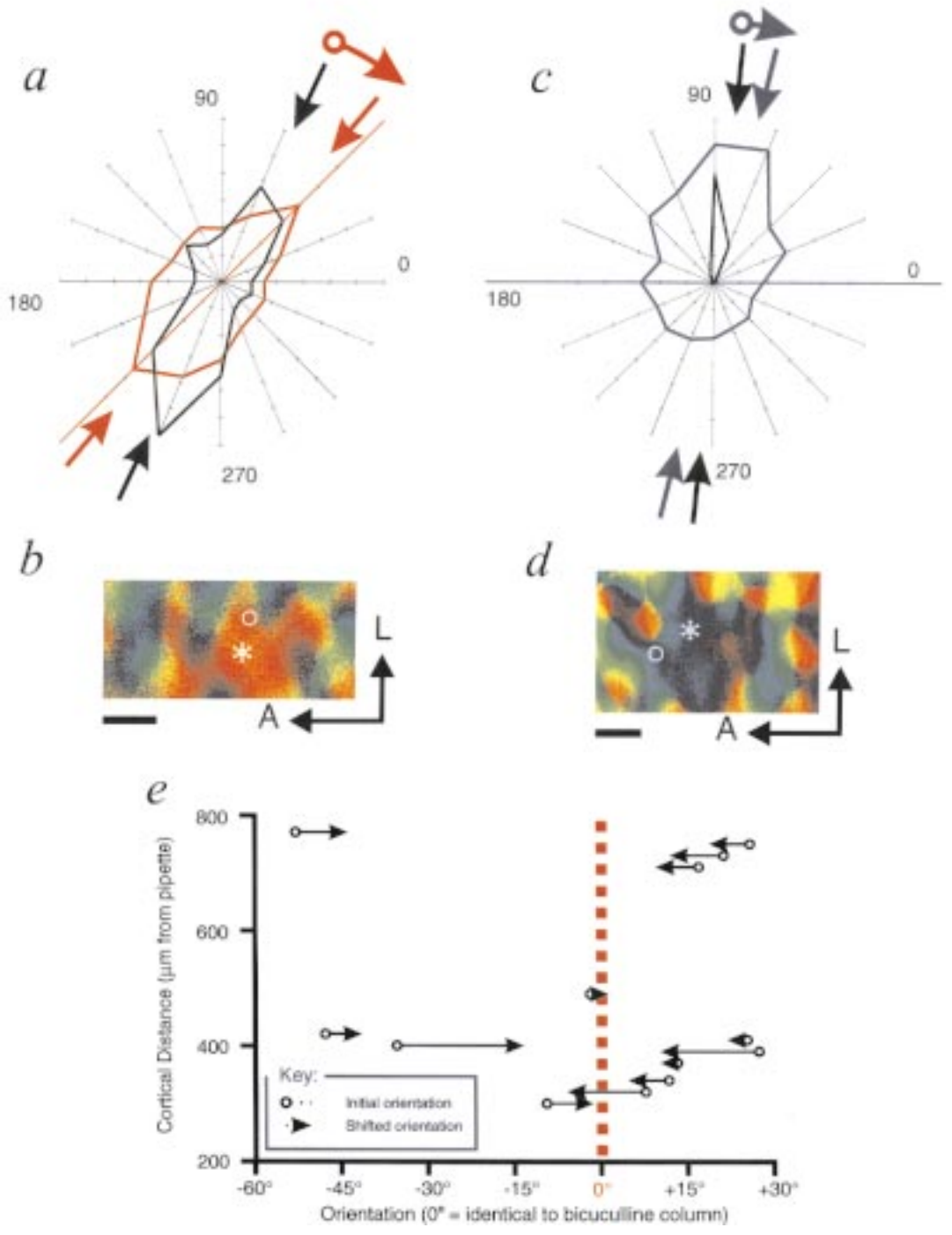

Figure 5. (*a*,*c*) Two single unit tuning curves (in polar form) from two different experiments are shown both before (black curves) and during (colored curves) bicuculline iontophoresis. For these polar plots, radius represents magnitude of response and angle represents stimulus direction. The orientation vector average, shown by the arrows in (*a*) and (*c*), was calculated to quantify the shift in orientation tuning (curved arrow) during bicuculline iontophoresis. The orientation preference at the injection site is indicated by the colored line through the plot. Although the magnitude of the shift is small relative to that in the intrinsic signal map, both cells exhibit a shift of their orientation vector in the direction of θ_{BIC}, the orientation preference at the pipette location. Units were recorded from sites within 1 mm of the pipette. Radius of plot: (*a*) 3 spikes/s, (*c*) 60 spikes/s. (*b*,*d*) The neuron (°) and pipette (*) positions are marked relative to the vector angle map of orientation preference (same colors and methods as Fig. 2). Scale bar: 1 mm. (*e*) The population data for 13 cells recorded in this manner are plotted as a function of distance of the cell away from the iontophoresis pipette (accurate to within 25 μm). Importantly, all shifts in orientation, however small, occur in the direction *towards* θ_{BIC}. Also, the magnitude of the shift is not dependent on the distance of the cell from the recording pipette, suggesting that the observed effects are not due to a direct dose-dependent action of bicuculline.

(Chapman *et al.*, 1991; Reid and Alonso, 1995; Ferster *et al.*, 1996), though intracortical circuitry may still amplify responses, sharpen tuning (Douglas *et al.*, 1995; Somers *et al.*, 1995) or affect the temporal structure of tuning (Ringach *et al.*, 1997). The single unit data presented here suggest that altering the efficacy of local connections only affects the orientation response on a fine scale. The axis of preferred orientation, as measured from extracellularly recorded spiking activity, changes

much less than does the orientation vector obtained by imaging intrinsic signals, which are known to reveal subthreshold activity as well (Das and Gilbert, 1995; Moore *et al.*, 1996; Toth *et al.*, 1996).Interestingly, adding stimuli to the receptive field surround may also induce shifts in orientation preference on a similar scale (Gilbert and Wiesel, 1990; Levitt and Lund, 1997). These observations suggest that the visual cortex is capable of some degree of dynamic modulation of orientation tuning, achieved through adjustments in the local balance of excitation and inhibition. Furthermore, they suggest that significant independent sources of cortically processed visual information are available which might influence but not drive responses in cortical neurons.

The data presented here indicate that local connections provide strong excitatory inputs which are integrated non-linearly by postsynaptic neurons. The presence of numerically massive and (as has been shown in this study) potentially functional local excitatory networks may serve other computational tasks for which non-linear summation of local inputs is essential. One such task is the control of cortical response gain (Bonds, 1989; Carandini and Heeger, 1994; Somers *et al.*, 1995), in which cells maintain orientation preference and tuning despite widely varying levels of input activity.

Notes

Although theoretically, an increase in tuning width among a local population of neurons might also be observed optically as a reduction in the intrinsic signal orientation vector magnitude, in practice that measurement confounds several response properties, including overall response magnitude and signal-to-noise ratio that preclude comparisons of tuning width between conditions of different average activity levels. As can be seen in Fig. 3*a*, vector magnitudes obtained from imaging in the region of bicuculline iontophoresis are actually greatly increased. Similarly, vector magnitudes in the region of GABA iontophoresis (data not shown) are decreased. Since the activity levels differ between these cases, these magnitudes can not be directly used to ascertain tuning widths of the underlying neuronal populations.

Supported by N.I.H. EY07023 to M.S.

Address correspondence to Dr Louis J. Toth, Department of Neurobiology, Harvard Medical School, 220 Longwood Avenue, Boston, MA 02115, USA. E-mail: ljtoth@warren.med.harvard.edu.

References

Ahmed B, Anderson JC, Douglas RJ, Martin KAC, Nelson JC (1994) Polyneuronal innervation of spiny stellate neurons in cat visual cortex. J. Comp. Neurol. 341:39–49.

Anderson JC, Douglas RJ, Martin KAC, Nelson JC (1994a) Synaptic output of physiologically identified spiny stellate neurons in cat visual cortex. J Comp Neurol 341:16–24.

Anderson JC, Douglas RJ, Martin KAC, Nelson JC (1994b) Map of the synapses formed with the dendrites of spiny stellate neurons of cat visual cortex. J Comp Neurol 341:25–38.

Bonds AB (1989) Role of inhibition in the specification of orientation selectivity of cells in the cat striate cortex. Vis Neurosci 2:41–55.

Bonhoeffer T, Grinvald A (1991) Iso-orientation domains in cat visual cortex are arranged in pinwheel like patterns. Nature 353:429–431.

Carandini M, Heeger DJ (1994) Summation and division by neurons in primate visual cortex. Science 264:1333–1336.

Chagnac-Amitai Y, Connors BW (1989) Horizontal spread of synchronized activity in neocortex and its control by GABA-mediated inhibition. J Neurophysiol 61:747–758.

Chapman B, Zahs KR, Stryker MP (1991) Relation of cortical cell orientation selectivity to alignment of receptive fields of the geniculocortical afferents that arborize within a single orientation column in ferret visual cortex. J Neurosci 11:1347–1358.

Crook JM, Eysel UT (1992) GABA-induced inactivation of functionally characterized sites in cat visual cortex (area 18): effects on orientation tuning. J Neurosci 12:1816–1825.

Dalva MB, Katz LC (1994) Rearrangements of synaptic connections in visual cortex revealed by laser photostimulation. Science 265:255–258

Dalva MB, Weliky M, Katz LC (1995) Spatial patterns of inhibition in developing and adult visual cortex: implications for cortical processing. Soc Neurosci Abstr 21:1284.

Das A (1996) Orientation in visual cortex: a simple mechanism emerges. Neuron 16:477–480.

Das A, Gilbert CD (1995) Long-range horizontal connections and their role in cortical reorganization revealed by optical recording of cat primary visual cortex. Nature 375:780–784.

Douglas RJ, Koch C, Mohowald M, Martin KAC, Suarez HH (1995) Recurrent excitation in neocortical circuits. Science 269:981–985.

Ferster D (1986) Orientation selectivity of synaptic potentials in neurons of cat primary visual cortex. J Neurosci 6:1284–1301.

Ferster D, Chung S, Wheat H (1996) Orientation selectivity of thalamic input to simple cells of cat visual cortex. Nature 380:249–252.

Gilbert CD, Wiesel TN (1989) Columnar specificity of intrinsic horizontal and corticocortical connections in cat visual cortex. J Neurosci 9:2432–2442.

Gilbert CD, Wiesel TN (1990) The influence of contextual stimuli on the orientation selectivity of cells in primary visual cortex of the cat. Vis Res 30:1689–1701.

Kamphuis W, Lopez da Silva FH (1990) The kindling model of epilepsy: the role of GABAergic inhibition. Neurosci Res Commun 6:1–10.

Katz LC, Callaway EM (1990) Development of local circuits in mammalian visual cortex. Annu Rev Neurosci 15:31–36.

Kim DS, Toth LJ, Rao SC, Sur M (1995) Orientation dynamics in adult visual cortex: focal infusion of bicuculline modifies optically imaged maps. Soc Neurosci Abstr 21:771.

Knierim JJ, VanEssen DC (1992) Neuronal responses to static texture patterns in area V1 of the alert macaque monkey. J Neurophysiol 67:961–980.

Levitt JB, Lund JS (1997) Contrast dependence of contixtual effects in primate visual cortex. Nature 387:73–76.

Markram H, Tsodyks M (1996) Redistribution of synaptic efficacy between neocortical pyramidal neurons. Nature 382:807–810.

Moore CI, Sheth BR, Basu A, Nelson S, Sur M (1996) What is the neuronal correlate of the optical imaging signal? Intracellular receptive field maps and optical imaging in rat barrel cortex. Soc Neurosci Abstr 22:1058.

Nelson SB, Toth LJ, Sheth BS, Sur M (1994) Orientation selectivity of cortical neurons during intracellular blockade of inhibition. Science 265:774–777.

Peters A, Jones EG, (1984) Visual cortex, Vol. 3: Cerebral cortex. New York: Plenum.

Pettigrew JD, Daniels JD (1973) Gamma-aminobutyric acid antagonism in visual cortex: different effects on simple, complex, and hypercomplex neurons. Science 182:81–83.

Ratzlaff EH, Grinvald A (1991) A tandem-lens epifluorescence macroscope: hundred-fold brightness advantage for wide-field imaging. J Neurosci Methods 36:127–137.

Reid RC, Alonso JM (1995) Specificity of monosynaptic connections from thalamus to visual cortex. Nature 378:281–284.

Ringach DL, Hawken MJ, Shapley R (1997) Dynamics of orientation tuning in macaque primary visual cortex. Nature 387:281–284.

Rockland KS and Lund JL (1982) Widespread periodic intrinsic connections in the tree shrew visual cortex. Science 215:1532–1534.

Rose D, Blakemore C (1974) Effects of bicuculline on functions of inhibition in visual cortex. Nature 249:375–377.

Sillito AM (1975) The contribution of inhibitory mechanisms to the receptive field properties of neurones in the striate cortex of the cat. J Physiol 250:305–329.

Sillito AM (1977) Inhibitory processes underlying the directional specificity of simple, complex and hypercomplex cells in the cat's visual cortex. J Physiol 271:699–720.

Sillito AM (1979) Inhibitory mechanisms influencing complex cell orientation selectivity and their modification at high resting discharge levels. J Physiol 289:33–53.

Sillito AM, Kemp JA, Milson JA, Berardi N (1980) A re-evaluation of the mechanisms underlying simple cell orientation selectivity. Brain Res 194:517–520.

Sillito AM, Grieve KL, Jones HE, Cudeiro J, Davis J (1995) Visual cortical mechanisms detecting focal orientation discontinuities. Nature 378:492–496.

Somers DC, Nelson SB, Sur M (1995) An emergent model of orientation selectivity in cat visual cortical simple cells. J Neurosci 15:5448–5465.
Stratford KJ, Tarczy-Hornoch K, Martin KAC, Bannister NJ, Jack JJB (1996) Excitatory synaptic inputs to spiny stellate cells in cat visual cortex. Nature 382:258–261.
Toth LJ, Kim DS, Sur M (1996) Do cortical cells integrate local inputs linearly? Short-range lateral interactions revealed by intrinsic signal and single-unit activity. Soc Neurosci Abstr 22:491.
Toth LJ, Kim DS, Rao SC, Sur M (1995) GABA iontophoresis modifies the intrinsic signal orientation map in cat area 18. Soc Neurosci Abstr 21:1655.
Toth LJ, Rao SC, Kim DS, Sur M (1996) Subthreshold facilitation and suppression in primary visual cortex revealed by intrinsic signal imaging. Proc Natl Acad Sci USA 93:9869–9874.
Toth LJ, Rao SC, Sur M (1994) Orientation-specific spread of activation in primary visual cortex measured by optical recording of intrinsic signals. Soc Neurosci Abstr 20:836.
Weliky M, Kandler K, Fitzpatrick D, Katz LC (1995) Patterns of excitation and inhibition evoked by horizontal connections in visual cortex share a common relationship to orientation columns. Neuron 3:541–552.